ACS OMEGA

http://pubs.acs.org/journal/acsodf

Article

Insight into the Loading and Release Properties of MCM-48/Biopolymer Composites as Carriers for 5-Fluorouracil: Equilibrium Modeling and Pharmacokinetic Studies

Mostafa R. Abukhadra,* Nermen M. Refay, Ahmed M. El-Sherbeeny,* and Mohammed A. El-Meligy

Cite This: *ACS Omega* 2020, 5, 11745−11755

Read Online

ACCESS | Metrics & More | Article Recommendations | Supporting Information

ABSTRACT: The effect of the integration between MCM-48 and some biopolymers (starch, chitosan, and β-cyclodextrin) on enhancing the pharmaceutical properties of MCM-48 as advanced carriers for the 5-fluorouracil drug was studied considering the loading capacities and the release profiles. The prepared carriers are MCM-48/chitosan (MCM/CH), MCM-48/starch composite (MCM/ST), and MCM-48/β-Cyclodextrin (MCM/CD). They emphasized excellent 5-Fu loading capacities of 141.2 mg/g (MCM-48), 156.6 mg/g (MCM/ST), 191 mg/g (MCM/CH), and 170 mg/g (MCM/CD), reflecting significant enhancement in the loading capacities. The kinetic and equilibrium investigation suggested physisorption loading of 5-Fu drug in a monolayer form for MCM-48, MCM/ST, and MCM/CH (Langmuir) and in a multilayer form for MCM/CD (Freundlich). This was supported by the estimated adsorption energies (0.23 kJ/mol (MCM-48), 0.26 kJ/mol (MCM/ST), 0.3 kJ/mol (MCM/CH), and 0.75 kJ/mol (MCM/CD)) and the thermodynamic parameters of free energy and enthalpy. The obtained release profiles for 80 h reflected significant controlling for the releasing behavior of MCM/48 on integrating its structure by adjusting the type of the selected polymer and its ratio. The pharmacokinetic modeling and the diffusion exponent from the Korsmeyer−Peppas model suggested non-Fickian transport behavior (a combination of erosion and diffusion releasing mechanism) for MCM/ST, MCM/CH, and MCM/CD and Fickian diffusion behavior (diffusion releasing mechanism) for MCM-48.

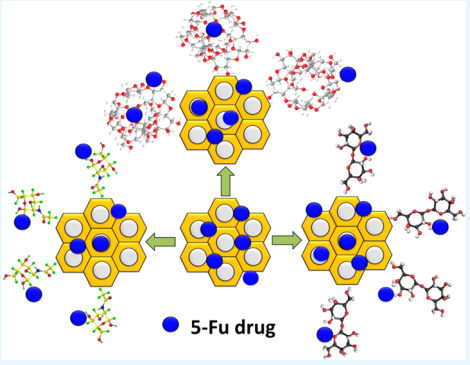

1. INTRODUCTION

Colorectal cancer is one of the widely distributed cancers and the main cause of death in several countries in the world, especially in developing countries.[1,2] Therefore, several types of therapies were introduced to mitigate the continuous increase in the number of patients in the world considering the production cost, efficiency of the products, biocompatibility, and safety properties.[3,4] Other techniques were discussed to improve or enhance the commonly used chemotherapies as 5-fluorouracil drugs. It is one of the most studied chemotherapies for cancer (pancreas, breast, colon, stomach, and rectum cancer).[5] However, 5-fluorouracil was signified as an effective anticancer drug and it suffers from several drawbacks and side effects. This is related to (a) its nonselectivity to the inherited cells, which can infect other fresh cells; (b) its toxicity effect when it is present in higher concentrations, especially in the cardiac, neural, hematological, and gastrointestinal tracts; and (c) the high diffusion rates of the drug molecules in the human body increasing the required dosages during the treatment periods.[1,6−8]

Therefore, the synthesis of advanced carriers for drug molecules with high technical and controlled-release properties was suggested to avoid the reported drawbacks of normal drug carriers.[4,9] Such promising drug carriers play a significant role in reducing the degradation rate of the drug, inducing its solubility, controlling the diffusing rate of the drug according to the therapeutic level, and enhancing the selectivity of the drug to the target inherited sites as well as its pharmacological and curative profiles.[3,4] Silica-based materials with mesoporous properties, such as MCM-41 and MCM-48, were introduced as effective adsorbents, catalyst carriers, and advanced delivery systems for different types of drugs.[10] This is related to their unique porous morphologies, significant thermal stabilities, very high surface area, and high reactive surfaces for the existence of the silanol groups.[11,12] The pharmaceutical value of such materials is mainly related to their biocompatibility and strong bonding with the adsorbed drug molecules by their functional groups.[13] Among the studied forms of mesoporous silica, MCM-48 was recommended as an effective material for different environmental and medical applications. MCM-48 is a common type of mesoporous silica with lamellar interwoven

Received: March 10, 2020
Accepted: May 5, 2020
Published: May 11, 2020

and branched porous structure, and this induces the mass transfer kinetics of the loaded drug molecules, which increase their loading capacities.[11]

The combination of MCM-48 and different types of biopolymers might result in advanced hybrid structures of promising biocompatibility, biodegradability, and high surface reactivity.[3] Starch, chitosan, and β-cyclodextrin are common biopolymers from natural resources and were investigated widely in different drug-delivery systems. Starch is one of the commonly studied natural polysaccharide polymers that are cheap and have high safety properties, significant biocompatibility, and excellent biocompatibility in addition to the availability of their natural resources.[14] For such technical properties, starch was applied widely in different medical and pharmaceutical applications including drug-delivery systems.[14] It was reported that starch-based drug carriers are valuable for inducing the solubility of the loaded drug, increasing the biocompatibility of the system, and reducing the predicted side effect of the drug.[15]

This was reported also for chitosan; it is a polyaminosaccharide natural polymer and exhibits high technical properties such as nontoxicity, bioactivity, mucoadhesivity, biodegradability, low immunogenicity, high biocompatibility, and outstanding loading capacity.[16,17] β-cyclodextrin biopolymer was recommended in the later periods in the synthesis of advanced drug carriers.[1] It has a torus-like structure from cyclic oligosaccharide units composed of seven glucose subunits (α-D) connected to each other by α-1,4-glucose bonds.[18,19] The inner surface of the β-cyclodextrin cavity shows lipophilic properties, while the outer surface shows hydrophilic properties, which induced its affinity to form strong complexes with various species of organic as well as inorganic ions.[1,20] β-cyclodextrin was investigated as a promising excipient material in different drug carriers, which enhanced the stability, solubility, and oral bioavailability of the loaded drug.[21,22]

This study evaluates three types of nanoporous silica/biopolymer composites, MCM-48/starch (MCM/ST), MCM-48/chitosan (MCM/CH), and MCM-48/β-cyclodextrin composite (MCM/CD), as novel carriers for a 5-fluorouracil drug with excellent loading capacities and controlled-release behaviors. The loading mechanisms and releasing behaviors were investigated considering the different kinetic, equilibrium, and pharmacokinetic studies. Additionally, the cytotoxicity of the composites before and after loading them by the 5-fluorouracil drug was investigated and discussed in the study.

2. RESULTS AND DISCUSSION

2.1. Characterization of the Carriers. *2.1.1. X-ray diffraction (XRD) Analysis.* The crystalline properties of MCM-48 and the introduced composites were studied from their low-angle and high-angle XRD patterns. The low-angle patterns demonstrated the successful synthesis of MCM-48, which is concluded from the detected peaks at (211) and (220) that characterize the mesoporous silica of the Ia3d space group and cubic porous structure[11] (JCPDS 00-049-171) (Figure 1A). After the successful combination of MCM-48 and the selected biopolymers (starch, chitosan, and β-cyclodextrin), their obtained low-angle pattern still displayed characteristic peaks of MCM-48 but with a notable decrease in their intensities (Figure 1B–D). This might be related to the integration of the polymers as a coating surface for MCM-48 or as pore-filling materials.

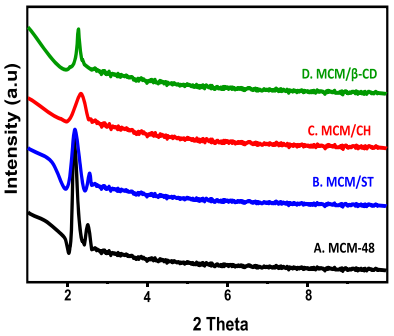

Figure 1. Low-angle XRD patterns of MCM-48, MCM/ST, MCM/CH, and MCM/CD.

The high-angle pattern of pure MCM-48 displayed a broad peak of noncrystalline silica at 22.5° that is known for mesoporous silica (Figure 2A).[11] The observed pattern for

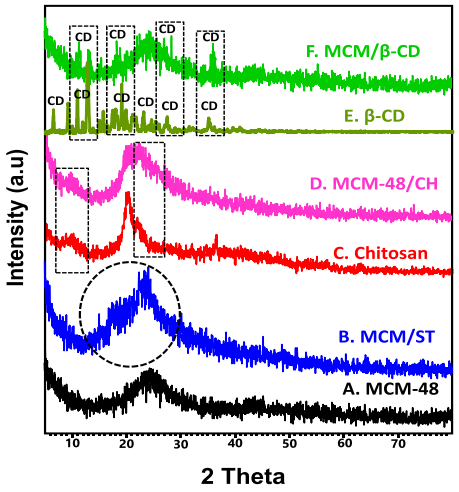

Figure 2. High-angle XRD patterns of MCM-48 (A), MCM/ST (B), chitosan (C), MCM/CH (D), β-cyclodextrin (E), and MCM/CD (F).

MCM/ST differs from the pattern of MCM-48 in the detection of three humps that were identified to be related to the combined starch chains (JCPDS 053-1663). This was supported by the reported deviation for the broad peak of MCM-48 from its previously identified position (Figure 2B). The MCM/CH XRD pattern (Figure 2D) showed a broad peak of MCM-48 in addition to two other peaks related to the chitosan polymer at 9.91 and 20.22° (JCPDS 39-1894) (Figure 2C).[11] This confirms the successful formation of a hybrid structure from chitosan and MCM-48. This was reported also for the pattern of MCM/β-CD (Figure 2F), which showed the main peak of mesoporous silica in addition to some peaks related to the β-cyclodextrin polymer, which is supported by comparing the pattern with that of pure β-cyclodextrin (JCPDS 17-1024) (Figure 2E).[1]

2.1.2. Scanning Electron Microscopy (SEM) and Transmission Electron Microscopy (TEM) Analyses. The SEM images of the synthetic MCM-48 confirm its successful synthesis with homogeneous elliptical or spherical grains in the agglomerated form as the characteristic morphology (Figure 3A). The integration between starch and MCM-48 (MCM/ST) resulted in cemented sheets from the synthetic mesoporous silica (Figure 3B). This reflected the role of the

https://dx.doi.org/10.1021/acsomega.0c01078
ACS Omega 2020, 5, 11745−11755

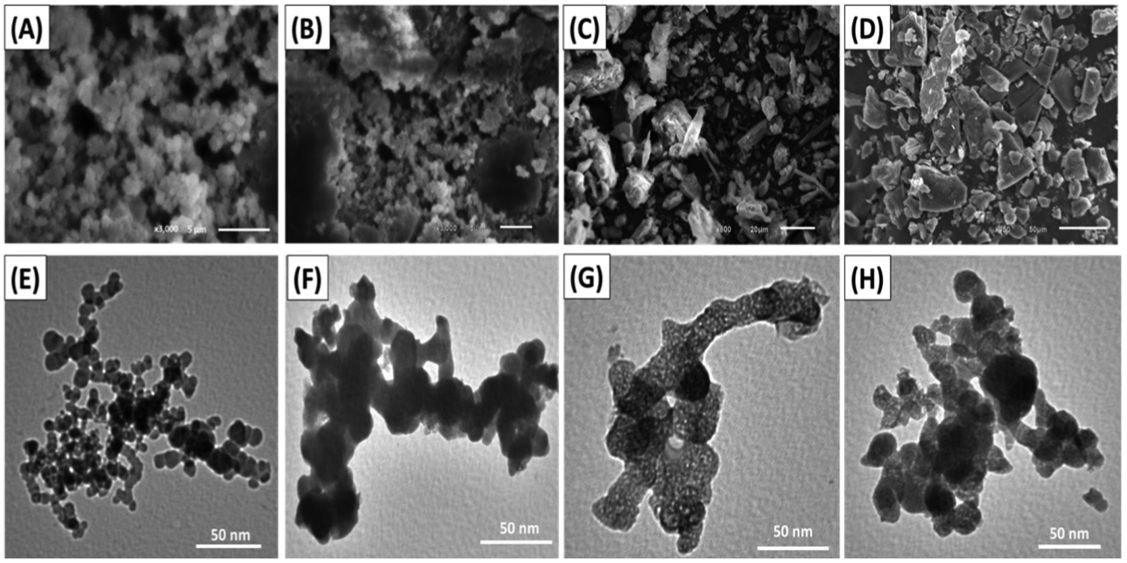

Figure 3. SEM images of MCM-48 (A), MCM/ST (B), MCM/CH (C), and MCM/β-CD (D). TEM images of MCM-48 (E), MCM/ST (F), MCM/CH (G), and MCM/CD (H).

starch gel in agglomerating the MCM-48 grain to each other (Figure 3B). The formation of composite from chitosan and MCM-48 (MCM/CH) resulted in the observable disappearance of the characteristic spherical grains of MCM-48 (Figure 3C). The composite appeared as longitudinal or lenticular particles of the chitosan chains, and MCM-48 might be enclosed within them (Figure 3C). The SEM images of MCM/β-CD displayed its formation as blocky or flakey grains without observation of the MCM-48 grains reflecting the enclave of the particles within the polymer matrix (Figure 3D).

The TEM images confirm the morphology previously identified in the SEM image. The particles were detected in their spherical form, and their aggregation resulted in a dendritic structure with several branches with their intersection forming the porous matrix (Figure 3E). The MCM/ST composite appeared in the TEM image as enlarged particles in the agglomerated form in an indefinite form (Figure 3F). The structure of MCM/CH in the TEM images reflected the encapsulation of the synthetic MCM-48 particles within the tubes of chitosan polymer, providing the final product with an outstanding porous structure (Figure 3G). The TEM image of the MCM/β-CD composite suggested cementation of the MCM-48 grains by the β-CD matrix forming enlarged particles with nearly spherical morphologies with significant detection of the porous structures of the coated MCM-48 (Figure 3H). This reflected on the textural properties of products, especially the surface areas that were measured to be 530, 423, 587, and 544 m^2/g for MCM-48, MCM/ST, MCM/CH, and MCM/CD, respectively.

2.1.3. Chemical Properties. The Fourier-transform infrared (FT-IR) spectra of MCM-48 and the synthetic composites are grouped in Figure 4. The spectrum of MCM-48 is the typical FT-IR spectrum of mesoporous silica with notable bands at about 465 cm^{-1} (Si−O bending of mesoporous silica), 1088 cm^{-1} (asymmetrical Si−O−Si), 796 cm^{-1} (symmetrical Si−O−Si), 1644 cm^{-1} (silanol groups), and 3433 cm^{-1} (adsorbed water molecules)[23,24] (Figure 4A).

The MCM/ST composite showed an FT-IR spectrum similar to that of MCM-48 with considerable intensification for the absorption bands at 3428 and 1640 cm^{-1} attributed to the

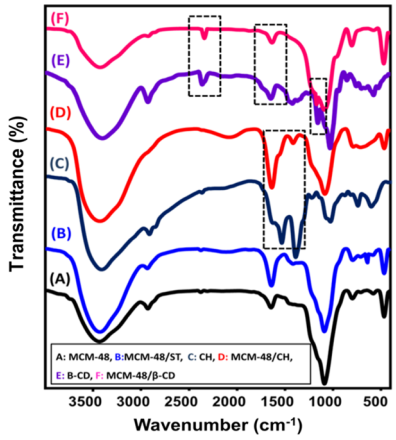

Figure 4. FT-IR spectra of MCM-48 (A), MCM/ST (B), chitosan (C), MCM/CH (D), β-cyclodextrin (E), and MCM/β-CD (F).

adsorbed water and silanol groups in MCM-48, respectively (Figure 4B). This might be assigned to the predicted overlapping between such groups and the functional groups of starch (O−H and C−O groups).[25,26] This was reported also for the detected band at 1089 cm^{-1} that might reflect the overlap between the C−O−H bending in starch and Si−O−Si bending of MCM-48.[27] The presence of starch was strongly supported by the observed band at about 622 cm^{-1} that signifies the present C−O−C ring of carbohydrates.[26]

Comparing the spectrum of MCM/CH with the spectra of pure chitosan, the pure chitosan phase reflected the presence of its main groups at 3423 cm^{-1} (O−H), 3423 and 1547 cm^{-1} (N−H), 2915 cm^{-1} (C−H), 1637 cm^{-1} (C═O), 1402 cm^{-1} (C−N), and 1040 cm^{-1} (C−O) (Figure 4C).[3] As detected in the MCM/ST composite, the MCM/CH composite displayed a spectrum similar to that of MCM-48 with observable intensification of the bands at about 3433 and 1638 cm^{-1} (Figure 4D). This was assigned to the predicted overlap between the previously mentioned functional groups of chitosan and MCM-48 at the same positions. The identification of the C−N bending related to chitosan in the

https://dx.doi.org/10.1021/acsomega.0c01078
ACS Omega 2020, 5, 11745−11755

spectrum of the composite at 1416 cm^{-1} supports the successful combination of MCM-48 and chitosan (Figure 4D).

The spectrum of the β-CD polymer showed the presence of O−H, asymmetrical C−H, polysaccharide C−C, hyperfine C−H, and symmetrical stretching of C−O and C−O−C in polysaccharides at 3376, 2926, 1666, 1482−1158, and 1000−1200 cm^{-1}, respectively (Figure 4E).[1,28,29] The obtained FT-IR spectrum of MCM/β-CD demonstrated the existence of different functional groups related to both the MCM-48 and β-CD polymer confirming the formation of the composite (Figure 4F).

2.2. 5-Fu Loading Properties and Mechanisms. *2.2.1. Loading Properties. 2.2.1.1. Loading Behavior with Different Time Intervals.* The influence of loading interval was studied after adjusting other loading conditions: 25 mg as the dosage for the applied carriers, 200 mg/L as the fixed concentration of the dissolved 5-Fu, pH 6, and 25 °C as the loading temperature (Figure 5A). The obtained loading curves

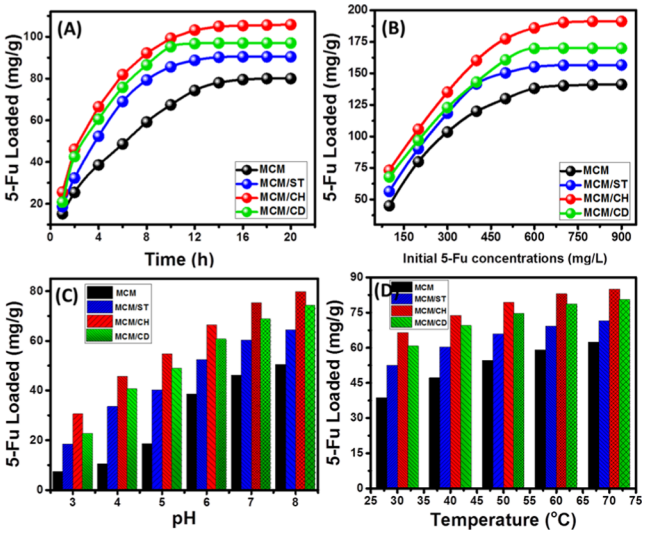

Figure 5. Effect of loading factors on the loading capacities of MCM/48 and the prepared biopolymer composites: (A) loading time interval, (B) concentration of the 5-Fu drug, (C) pH of the drug aqueous solution, and (D) loading temperature.

as a function of the selected loading intervals for MCM-48 and the produced composite demonstrated a considerable increase in the loading quantity with time until reaching a stable state in the loading quantities of 5-Fu, which can be identified as the equilibrium state (Figure 5A). The reported loading equilibrium times are 14, 12, 10, and 14 h for MCM-48, MCM/ST, MCM/CH, and MCM/CD, respectively (Figure 5A). The reported equilibrium loading capacities are 80, 90.4, 106, and 97 mg/g for MCM-48, MCM/ST, MCM/CH, and MCM/CD, respectively (Figure 5A).

The reported increase in the quantities of the loaded 5-Fu by MCM-48 and the produced composites is associated with the observable decrease in their loading rates. This is a normal behavior in most of the studied loading systems and related to the systematic occupation of active sites of the assessed carrier with time until their full saturation.[3] According to the estimated results, the integration between mesoporous silica and such carbohydrate biopolymers has a strong impact in enhancing the loading properties of the 5-Fu drug. This might be assigned to the resulting heterogeneous structures that have enhanced surface properties, complex and new functional groups, and high affinity of the polymers for the organic molecules of the studied drug. The reported high loading capacities of MCM/CH compared to those of MCM/CD and MCM/ST in order might be related to its higher surface area and the resulting new porous structure after the integration process.

2.2.1.2. Loading Behavior with Different 5-Fu Concentrations. The investigation of loading capacities using different 5-Fu concentrations was performed at 24 h as equilibrium interval using 25 mg as the dosage of the carriers at pH 6 and 30 °C loading temperature (Figure 5B). The results demonstrated that the investigated MCM-48 and the prepared biopolymer composites achieved high loading capacities with the incorporation of high 5-Fu concentrations, reflecting the possible control of the loading quantities (Figure 5B). This can be detected until the investigation of a 5-Fu concentration of 600 mg/L for the four carriers that was identified as the equilibrium concentration (Figure 5B). The experimental maximum loading capacities of MCM-48, MCM/ST, MCM/CH, and MCM/CD are 141.2, 156.6, 191, and 170 mg/g, respectively (Figure 5B). These values also higher than the values obtained for the integrated polymer at the same conditions as the estimated capacities of starch, chitosan, and β-cyclodextrin are 5.3, 12.4, and 8.7 mg/g, respectively. The observed increase in the loading quantities of 5-Fu by the assessed carriers was assigned to the expected inducing for the driving forces of 5-Fu molecules with testing high concentrations of it.[3] Moreover, the detected curves are of 2L-type equilibrium curves that commonly formed with the materials with excellent affinity for the studied dissolved drug molecules.[3]

2.2.1.3. Loading Behavior with Different pH Values. The predicted effect of pH on controlling the loading behaviors of the prepared MCM-48 and the composites was studied after fixation the following conditions: 4 h as loading time, 200 mg/L as 5-Fu concentration, 25 mg as the dosage of the carriers, and 30 °C as the loading temperature (Figure 5C). The results demonstrated intensification in the loaded quantities by the carriers with a systematic increase in the adjusted pH from 3 to 8 (Figure 4B) (Figure 5C). The best loading pH value is pH 8, and the achieved loading capacities at this pH are 50.5, 64.5, 79.8, and 74.2 mg/g for MCM-48, MCM/ST, MCM/CH, and MCM/CD, respectively (Figure 5C). This behavior might be attributed to the surface specification of the carriers as well as the dissolved drug molecules. The deprotonation of the present functional groups of the carriers induced electrostatic attractions between their negatively charged surfaces and the drug molecules.[23] This is supported by the ionization of the dissolved 5-Fu drug molecules (pK_1 = 8) at a reaction pH of 5.5, which induced such interactions.[36] This is also supported by the measured pH values of the zero point charge (pH (PZC)) for MCM (pH (PZC) = 6.6), MCM/ST (pH (PZC) = 5.8), MCM/CH (pH (PZC) = 6.7), and MCM/CD (pH (PZC) = 6.5), i.e., the materials have negative charges above these values.

2.2.1.4. Loading Behavior with Different Loading Temperature Values. The loading behavior of 5-Fu by MCM-48 and the prepared composites as a function of loading temperature was assessed at a loading time of 4 h, pH 6, carrier dosage of 25 mg, and drug concentration of 200 mg/L (Figure 5D). The reported increment in the loading capacities of MCM-48, MCM/ST, MM/CH, and MCM/CD for 5-Fu drug with the

https://dx.doi.org/10.1021/acsomega.0c01078
ACS Omega 2020, 5, 11745−11755

systematic increase in the loading temperature reflected the endothermic properties of the studied materials as drug-delivery systems (Figure 5D). The obtained loading capacities at 70 °C, the best loading temperature, are 62.4, 71.6, 85, and 80.4 mg/g for MCM-48, MCM/ST, MM/CH, and MCM/CD, respectively (Figure 5D). The obtained results demonstrated that the integration between nonporous silica of MCM-48 structure and the reported carbohydrate polymers resulted in the hybrid structure of promising properties as drug-delivery systems, in which the quantities of the loaded drug can be controlled by adjusting the loading factors.

To confirm the successful entrapment of the 5-Fu molecules within the structures of the prepared carriers, the FT-IR spectra of the carriers obtained after the loading processes were evaluated and are presented in Figure 6. The obtained spectra

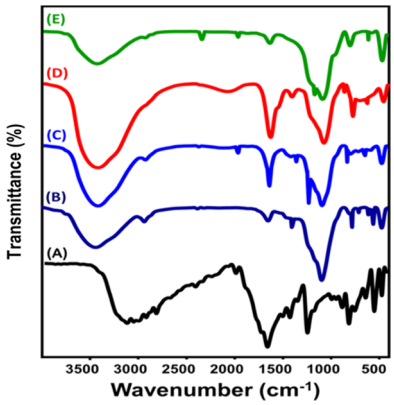

Figure 6. FT-IR spectra of 5-Fu drug (A), MCM-48 loaded by 5-Fu (B), MCM/ST loaded by 5-Fu (C), MCM/CH loaded by 5-Fu (D), and MCM/CD loaded by 5-Fu drug (E).

demonstrated the existence of the previously reported functional groups of the prepared carriers in addition to new bands related to the functional groups of 5-Fu drug molecules. The most detected groups are the C═O group related to the ester as well as the carboxylic acids (1721 cm^{-1}), C═F group (1263.4 cm^{-1}), CF═CH (754 cm^{-1}), and NH− group (546 cm^{-1})[1] (Figure 6).

2.2.2. Loading Kinetic, Equilibrium, and Thermodynamic Properties. 2.2.2.1. Kinetic Behavior. The kinetic behaviors of the loading processes for the prepared carriers of MCM-48, MCM/ST, MCM/CH, and MCM/CD were described considering the hypothesis of both the pseudo-first-order model and pseudo-second-order kinetic (Figure 7A). The illustrative equations of these models are reported in Table S1, and the fitting processes were accomplished through the nonlinear fitting. The theoretical parameters of the fitting results, as well as the correlation coefficient values, are shown in Table 1. However, the loading results of 5-Fu by all of the prepared carriers showed significant agreement with both pseudo-first-order and pseudo-second-order models, and the kinetic properties of the studied systems showed a slight preference to be explained according to the hypothesis of the pseudo-first-order model (Figure 7A and Table 1). This reflected the dominance of the physisorption mechanisms during the loading of 5-Fu molecules, and the signified fitting with the pseudo-second-order model suggested the operation of other assistance mechanisms that have more chemical affinity. The suggested assistance mechanisms might involve internal diffusion, surface complexation, electron exchange, and electron sharing.[30]

2.2.2.2. Equilibrium Modeling. The equilibrium behaviors and the isotherm properties were discussed based on the nonlinear fitting results with Langmuir and Freundlich models as well as the Dubinin−Radushkevich model (Figure 7B−E). The illustrative formulations of the models and their theoretical parameters from the nonlinear fitting processes are shown in Tables S1 and 1, respectively. The loading properties of MCM-48, MCM/ST, and MCM/CH showed excellent agreement with both Langmuir and Freundlich models but with a preference for the Langmuir model,

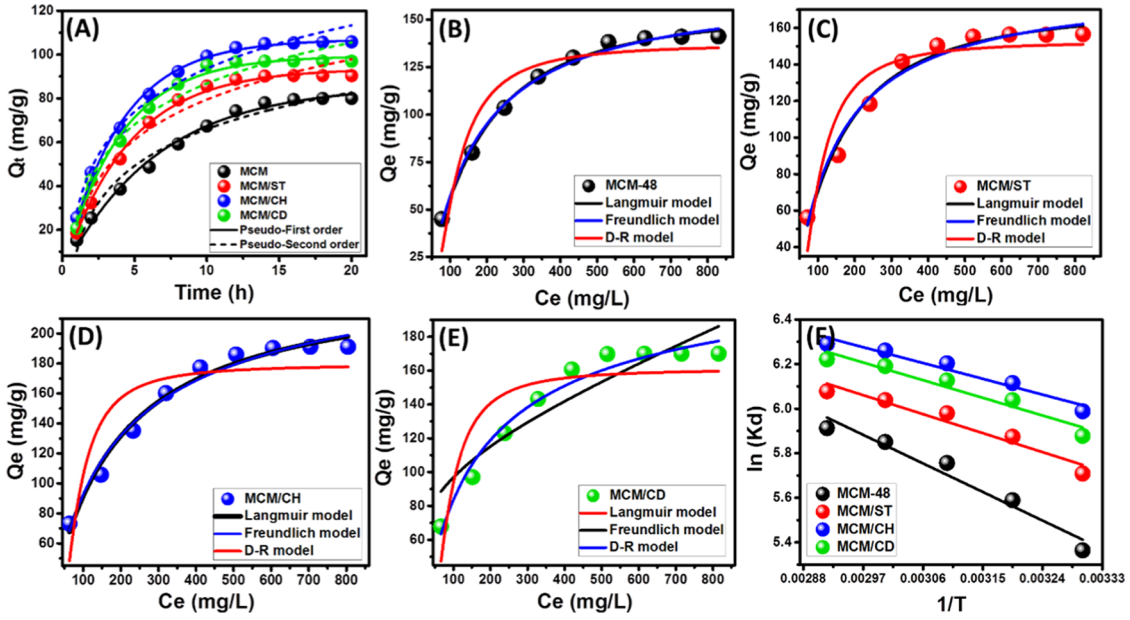

Figure 7. Nonlinear fitting of the loading results with the kinetic models (A), fitting of MCM-48 loading results with the isotherm models (B), fitting of MCM/ST loading results with the isotherm models (C), fitting of MCM/CH loading results with the isotherm models (D), fitting of MCM/CD loading results with the isotherm models (E), and fitting of the loading results with the van't Hoff equation (F).

https://dx.doi.org/10.1021/acsomega.0c01078
ACS Omega 2020, 5, 11745−11755

Table 1. Theoretical Parameters of the Studied Kinetic, Isotherm, and Thermodynamic Studies

model	parameters	MCM-48	MCM-48/ST	MCM-48/CH	MCM-48/β-CD
Kinetic Models					
pseudo-first order	K_1 (mg/min)	0.153	0.221	0.256	0.253
	$q_{e(Cal)}$ (mg/g)	85.8	93.6	106.9	99.4
	R^2	0.99	0.995	0.996	0.993
pseudo-second order	k_2 (mg/min)	0.014	0.038	0.035	0.037
	$q_{e(Cal)}$ (mg/g)	87.3	94.8	112.3	101.5
	R^2	0.97	0.96	0.97	0.95
Isotherm Models					
Langmuir	q_{max} (mg/g)	156.6	173.13	238.7	183
	b (L/mg)	7.22×10^{-4}	0.001×10^{-4}	0.0065	2.4
	R^2	0.994	0.98	0.98	0.82
	X^2	0.57	2.72	4.3	12.4
	R_L	0.61−0.93	0.99	0.145−0.61	0.004−0.0046
Freundlich	$1/n$	0.89	0.81	1.28	1.24
	k_F	168.2	184.2	270	234.12
	R^2	0.991	0.97	0.97	0.96
	X^2	0.96	3.68	5.13	5.1
D−R model	β (mol^2/KJ^2)	9.62	7.28	5.35	0.88
	q_m (mg/g)	137	152.7	179.8	160.9
	R^2	0.90	0.86	0.76	0.75
	X^2	12.3	18.2	17.4	13.4
	E (kJ/mol)	0.23	0.26	0.3	0.75
Thermodynamic Parameters					
ΔG° (kJ/mol)	303 K	−13.5	−14.4	−15.1	−14.81
	313 K	−14.5	−15.3	−15.9	−15.7
	323 K	−15.46	−16.05	−16.7	−16.45
	333 K	−16.2	−16.72	−17.3	−17.14
	343 K	−16.86	−17.3	−17.94	−17.74
ΔH° (kJ/mol)		11.83	7.86	6.55	7.31
ΔS° (J/(K mol))		83.97	73.74	71.6	73.32

considering the values of the determination coefficient and chi-square (χ^2) (Figure 7B−D and Table 1). This suggested monolayer loading for the 5-Fu drug molecules by homogeneous active sites on the surface of the presented carriers. The reverse was reported for the loading of 5-Fu molecules by MCM/CD, and the results demonstrated an exceptional fit with the Freundlich model and a medium fit with the Langmuir model, i.e., this system involved a heterogeneous loading process of the multilayer form[3] (Figure 7E and Table 1). The obtained theoretical maximum loading capacities for the reported carriers considering the Langmuir model are 156.6 mg/g (MCM-48), 173.13 mg/g (MCM/ST), 238.7 mg/g (MCM/CH), and 183 mg/g (MCM/CD) (Table 1). Additionally, the estimated RL values demonstrated favorable loading (lower than 1) for 5-Fu by MCM-48, MCM/ST, MCM/CH, and MCM/CD (Table 1).[1]

Fitting of the loading results with the Dubinin−Radushkevich (D−R) model to predict the nature of the loading mechanism, either chemical or physical, depends on the values of the Gaussian energy.[31] The loading energies which were calculated for the loading of 5-Fu by MCM-48, MCM/ST, MCM/CH, and MCM/ CD are 0.23, 0.26, 0.3, and 0.75 kJ/mol, respectively (Table 1). The estimated values reflected the physisorption loading mechanisms for the investigated carriers, which can be supported by the previously investigated kinetic models.[32]

2.2.2.3. Thermodynamic Properties. The thermodynamic evaluation for the loading process of 5-Fu by MCM-48 and the prepared biopolymer composites involved the determination of the Gibbs free energies (ΔG°) in addition to the enthalpies (ΔH°) and entropies (ΔS°) of the performed loading reactions. The Gibbs free energies were calculated by its normal formulation (eq 1), while the values of both ΔS° and ΔH° were calculated as theoretical parameters for the fitting of the loading results with the van't Hoff equation (eq 2) (Figure 7F and Table 1).

$$\Delta G^0 = -RT \ln K_c \quad (1)$$

$$\ln(K_c) = \frac{\Delta S^\circ}{R} - \frac{\Delta H^\circ}{RT} \quad (2)$$

All of the ΔG° values were detected with negative sign, reflecting the spontaneous loading processes by the assessed carriers with an observable decline in the favorability of the conducted loading reactions at higher loading temperature values[33] (Table 1). The values of ΔH° were obtained with positive sign, suggesting endothermic loading reactions for the prepared carriers (Table 1). Moreover, the detection of ΔS° as positive values suggested intensification in the randomness of the operating loading reactions (Table 1). The calculated values of both ΔG° and ΔH° are related to physisorption loading processes, which are in agreement with kinetic and isotherm studies.

2.3. In Vitro Release Profiles. The obtained releasing curves for MCM-48, MCM/ST, MCM/CH, and MCM/CD in the inspected buffers (gastric fluid (pH 1.2) and intestinal fluid (pH 7.4)) showed two notable segments for the released 5-Fu representing two different release rates (Figure 8). These

https://dx.doi.org/10.1021/acsomega.0c01078
ACS Omega 2020, 5, 11745−11755

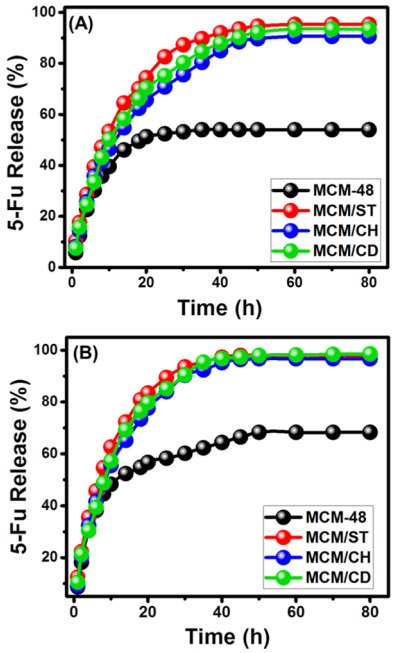

Figure 8. Release profile of 5-Fu from MCM-48, MCM/ST, MCM/CH, and MCM/CD in gastric fluid (pH 1.2) (A) and intestinal fluid (pH 7.4) (B).

release rates can be signified as a stage of rapid change in the diffusion rates, followed by the second state of slight or nearly fixed release rates demonstrating the attainment of equilibrium states (Figure 8). The first stage reflected the fast diffusion of the absorbed 5-Fu or the adsorbed molecules by external receptor sites on the surface of the carriers. The second segment or the equilibrium stage demonstrated the final stage of the release process, which might be related to the slow diffusion of the entrapped 5-Fu molecules within the channels of MCM-48 and the matrix of the combined biopolymers (Figure 8).[1,34]

The release of 5-Fu from MCM-48 was inspected for 80 h, and the results validated a very slow release profile without complete diffusion for the loaded quantity either in the gastric fluid or in the intestinal fluid (Figure 8). The maximum release percentages are 54 and 68.3% in the acidic fluid and basic fluid, respectively, and such values were obtained after 35 and 50 h, respectively. Such a low release profile might be assigned to the expected strong hydrogen bonds between the loaded 5-Fu molecules and the dominant silanol functional groups of the synthetic MCM-48.[35] This hinders the effective release of the 5-Fu molecules from the MCM-48 structure, which prevents successful diffusion of the drug in the therapeutic level. The increase in the release rate of the intestinal fluid compared to the gastric fluid is related to the ionization of 5-Fu as the alkaline environments, which induce their dissolution and diffusion in the buffer solution.[35,36]

The prepared MCM-48/starch composite (MCM/ST) displayed faster release rates in both alkaline and acidic buffer solutions. In the gastric buffer solution (pH 1.2), the composite achieved released percentages of 50 and 95% after 10 and 60 h, respectively (Figure 8A). The release percentage was fixed at 95.3% without reporting for the complete release of the loaded 5-Fu (Figure 8A). In the basic buffer solution, the composite achieved release percentages of about 50 and 95% after 8 and 35 h, respectively, and the maximum released percentage is 98%, which did not change even after 80 h (Figure 8B).

The MCM-48/chitosan composite (MCM/CH) emphasized faster-release profiles than MCM-48 but slower than that reported for the MCM/ST composite. This related to the expected encapsulation of the 5-Fu molecules among the positively charged hydrophilic chains of chitosan.[3] Additionally, the diffusion of the loaded 5-Fu molecules from the integrated chitosan chains involved the first degradation for the polymeric matrix, which reduces the release rates.[36] In the gastric fluid, the composite demonstrated a release percentage of 50% after 14 h, and the maximum releasing value (90.6%) was obtained after 60 h, which did not change up to 80 h (Figure 8A). In the intestinal fluid, the release percentages of about 50 and 95% were recorded after 10 and 40 h, respectively. The release percentage was constant at 96.7% even after 80 h (Figure 8B).

This was reported also for MCM-48/β-Cyclodextrin (MCM/CD), which showed release percentages of 50% in the gastric buffer solution after 10 h, and the maximum release percentage (93.5%) was obtained after about 60 h without reporting for the complete diffusion for the loaded dosage (Figure 8A). In the intestinal buffer, the composite showed release percentages of about 50 and 95% after 8 and 35 h, respectively (Figure 8B). The maximum percentage of the released 5-Fu drug is about 98%, which did not change even after 80 h (Figure 8B). A reported increase in the release rate after the combination of MCM-48 and the selected biopolymers of starch, chitosan, and β-cyclodextrin related to their role as coating material or barriers between the silanol groups of mesoporous silica and the functional groups of the 5-Fu drug. This hindered the expected bonding between the drug molecules and the silanol groups by hydrogen bonds and in turn induced the diffusion of the 5-Fu molecules. Moreover, the homogeneous loading of the 5-Fu molecules with the matrix and chains of the polymers has a strong influence in accelerating the diffusion of the drug during the release tests.[37]

It was reported that the use of drug carriers with abrupt and very rapid release profiles might induce the diffusion of the drug at the required therapeutic concentrations within short intervals.[3] However, this also has negative impacts for the expected increase in the required dosages and the predicted random distribution for the diffused drug molecules. Also, the synthesis of carriers with very slow release profiles is of valuable impact in keeping the diffused drug concentration at its therapeutic value for long periods.[3,36] Therefore, the combination of MCM-48 and some healthy and safe biopolymers can result in advanced hybrid structures of promising loading and release properties as carriers for the 5-Fu drug. The quantities of the loaded drug can be controlled by adjusting the loading factors and type of the combined polymer. Also, the release rates and be controlled by adjusting the type of the integrated polymers as well as their ratio in the prepared composites.

2.4. Pharmacokinetics Behavior of the Releasing Results. The releasing mechanisms of 5-Fu from the prepared MCM-48 and the three composites as drug-delivery systems were evaluated based on the commonly introduced pharmacokinetic models. The investigated pharmacokinetic models are the zero-order model, the first-order model, the Higuchi model, the Hixson–Crowell model, and the Korsmeyer–Peppas kinetic model. This was accomplished by the linear

https://dx.doi.org/10.1021/acsomega.0c01078
ACS Omega 2020, 5, 11745−11755

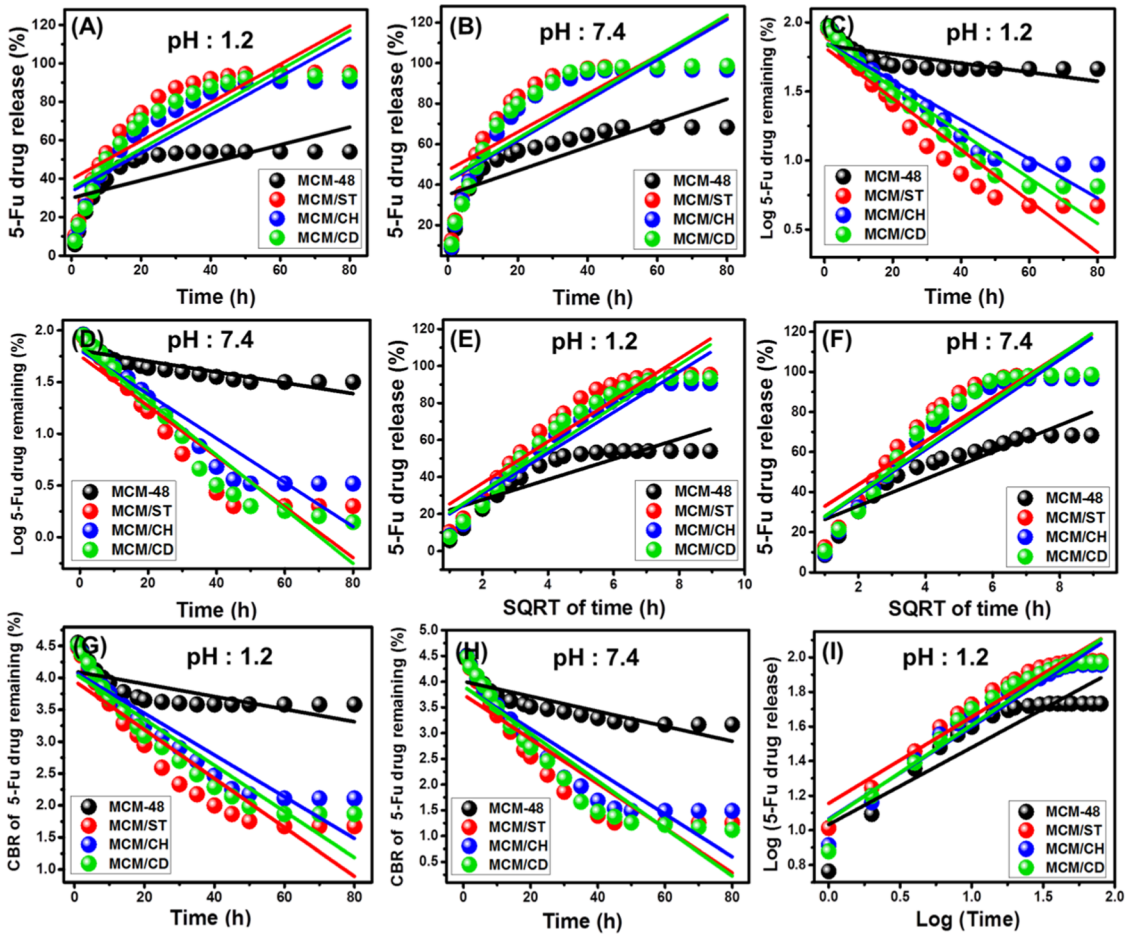

Figure 9. Fitting of the releasing results with pharmacokinetic models; (A, B) zero-order model, (C, D) first-order model, (E, F) Higuchi model, (G, H) Hixson–Crowell model, and (I) Korsmeyer–Peppas model.

fitting process with the linear formulations of the models as in eqs 3–7 for the previously reported models in order.[38]

$$W_t - W_0 = K_0 t \quad (3)$$

$$\ln(W_\infty / W_t) = K_1 t \quad (4)$$

$$W_t = K_h t^{1/2} \quad (5)$$

$$W_o^{1/3} - W_t^{1/3} = K_{HC} t \quad (6)$$

$$W_t / W_\infty = K_p t^n \quad (7)$$

According to the hypothesis of the zero-order model, the release of the drug molecules occurs at constant rates within the studied release without any effect on the concentration of the loaded molecules.[39] The first-order model was used mainly to describe the releasing behaviors that depend on the quantities of the loaded drug molecules.[1] Regarding the assumption of the Higuchi model, it represents drug-delivery systems in which release occurs through dissolution and diffusion mechanisms.[1] Fitting the releasing data with this model suggested that (a) the quantities of the loaded 5-Fu molecules are higher than their diffusion rates, (b) the diffusion of the loaded molecules is controlled by one direction only, (c) the diameters of the loaded drugs are smaller than the thickness of the used carriers, (d) the release rates were not affected by both the solubility and the swelling index of the integrated polymer matrix, (e) the systems of such kinetic properties are of constant diffusion rates, and (f) the releasing behavior reflected strong sink properties.[40,41]

The Hixson–Crowell model was used to illustrate the releasing systems in which the behavior depends on the diameters of the carriers and their surface area. This model suggested the occurrence of the diffusion process in parallel plane forms with a significant decrease in the dimensions of the prepared carriers. Additionally, this model suggested the existence of erosion as the dominant releasing mechanism.[3] The Korsmeyer–Peppas model was considered as the best model used to describe the drug-delivery systems that are of polymeric nature and of strong value in identifying the operating mechanism of diffusion, erosion, or their combination.[1]

The fitting degrees were estimated based on the calculated values of the correlation coefficient for the fitting results of the released 5-Fu drug from the synthetic biopolymer composites (Figure 9 and Table S1). As reported in Table S1, the releasing results of the four carriers show poor fit with the zero-order model (Figure 9A,B) compared to their fit with the first-order model (Figure 9C,D), especially for the investigated biopolymer composites. This demonstrated a significant dependence of their release behaviors on the quantities of the loaded 5-Fu molecules in acidic and basic buffers but with a preference for acidic conditions. This might be related to the role of acidic conditions in causing partial degradation of the polymeric chains.[3] The pure phase of MCM-48 displayed

https://dx.doi.org/10.1021/acsomega.0c01078
ACS Omega 2020, 5, 11745–11755

releasing behavior of poor fit with both zero-order and first-order kinetic models reflecting the role of the integrated biopolymers in directing the releasing mechanism of such mesoporous structures.

The obtained release data from MCM-48 showed good fit with the Higuchi model, and the degree of fitness increases systematically with the combination of MCM-48 with starch, chitosan, and β-cyclodextrin achieving the best fitting results with MCM/CH and MCM/CD in the gastric fluid (Figure 9E,F and Table S1). This suggested a strong diffusion mechanism for the released 5-Fu drug from the composites, especially for MCM/CH and MCM/CD in the acidic conditions. This also reflected the strong role of the diffused 5-Fu molecules from the structural cavities of MCM-48 as an advanced silica base material of mesoporous nature.

The Hixson−Crowell model has low fitting results with the obtained releasing data of MCM-4, while the composites have a medium to very good fit with this model, especially in the acidic buffer for MCM/CH and MCM/CD (Figure 9G,H and Table S1). The calculated determination coefficient values for this model are lower than the reported values with both the first-order model and the Higuchi model (Table S2). This reflected the possible control of the release profiles of the studied carriers by erosion and diffusion mechanisms with dominance for the diffusion mechanism.

For all of the investigated pharmacokinetic models, the obtained releasing data from all of the carriers either in the gastric fluid or in the intestinal fluid achieved the best fit with the Korsmeyer−Peppas model. The calculated diffusion exponent (n) values in the intestinal fluid are 0.4, 0.45, 0.49, and 0.48 for MCM-48, MCM/ST, MCM/CH, and MCM/CD, respectively (Figure 9I and Table S1). The reported values in the gastric fluid are 0.45, 0.5, 0.53, and 0.55 for the same carriers in order. Such results demonstrated that the release of 5-Fu from MCM/CH and MCM/CD shows non-Fickian transport behaviors in acidic and basic conditions, which involved both erosion and diffusion mechanisms.[3] The release profile of MCM-48 either in the acidic fluid or basic fluid shows Fickian diffusion behavior (Case I diffusion), which suggested controlling the process by the diffusion mechanism. For MCM/ST, its release profile in the basic conditions shows non-Fickian transport behavior and that in the acidic condition shows Fickian diffusion behavior.

3. CONCLUSIONS

The MCM-48/chitosan (MCM/CH), MCM-48/starch (MCM/ST), and MCM-48/β-Cyclodextrin (MCM/CD) composites were prepared as carriers for the 5-Fu drug with enhanced loading and releasing properties. The calculated loading capacities are 141.2, 156.6, 191, and 170 mg/g for MCM-48, MCM/ST, MCM/CH, and MCM/CD, respectively. The loading process by MCM-48, MCM/ST, and MCM/CH is of physisorption type and monolayer form, while the loading by MCM/CD occurs in a multilayer form considering the results of kinetic, isotherm, and thermodynamic studies. The release profiles from 80 h indicated the possible control of the release rate by adjusting the type of the integrated polymer and its ratio. The diffusion exponent from the Korsmeyer−Peppas model indicated a combination of erosion and diffusion mechanisms for the release of 5-Fu from MCM/ST, MCM/CH, and MCM/CD and the diffusion releasing mechanism from MCM-48.

4. EXPERIMENTAL SECTION

4.1. Materials. Cetyltrimethylammonium bromide (99%), tetraethylorthosilicate (97%), ethanol (95%), ammonium solution (30% NH_3), and NaOH pellets (97%) were delivered by Sigma-Aldrich, Egypt, for the fabrication of MCM-48. Chitosan polymer, nonsoluble starch (wheat), and β-cyclodextrin polymer of high-purity grades were incorporated in the synthesis of the MCM-48/biopolymer composites.

4.2. Preparation of MCM-48/Biopolymer Composites.

4.2.1. Synthesis of MCM-48. The synthesis procedures were accomplished by the sol−gel method. The typical steps involved first dissolving about 29.74 g of the surfactant template (CTAB) in about 146.88 g of distilled water. This was followed by the addition of NaOH (2.72 g) under stirring at 500 rpm for 15 min. Then, about 30 mL of TEOS was added to the mixture as the main source of silica and stirred for another 180 min at a fixed temperature of 40 °C. After that, the mixture was put into a sealed Teflon reactor and heated at 110 °C for 24 h. After thermal treatment, the synthesized MCM-48 particles were filtered, washed thoroughly with ethanol and distilled water, and dried for 8 h at 60 °C. The final synthesis step involved thermal treatment of the solid fractions at 550 °C for about 6 h to remove the used surfactant template and open the pores of the structure.

4.2.2. Synthesis of MCM-48/Biopolymer Nanocomposite. The first separated colloid solutions for the studied biopolymers were prepared as separated samples (starch, chitosan, and β-cyclodextrin). The starch colloid solution was prepared by direct dissolving of about 3 g of starch within about 50 mL of distilled water at 90 °C for 60 min. The chitosan gel was prepared by normal dissolving of 3 g of the polymer within 50 mL of diluted acetic acid. Also, the β-cyclodextrin solution was prepared by dissolving 3 g of it within 50 mL of the ethanol/water mixture (50:50%). At the same time, three samples of MCM-48 suspensions were prepared by dispersion of MCM-48 solid fractions (3 g) in distilled water (50 mL) and mixed homogeneously for 2 h as separate tests. After that, the polymer-bearing solutions were mixed with the above MCM-48 mixtures under a complex system of stirring (800 rpm) and sonication (240 W) as the effective mixing system for 12 h at room temperature for MCM-48/chitosan (MCM/CH) and MCM-48/β-cyclodextrin composite (MCM/CD) and at 70 °C for MCM-48/starch (MCM/ST). Finally, the prepared composites were separated, washed, and dried for 12 h at 60 °C.

4.3. Characterization Techniques. The crystalline phases were evaluated considering the XRD patterns of the synthetic materials by a PANalytical X-ray diffractometer (Empyrean). The integration process was also confirmed based on the functional groups of the synthetic materials using an FT-IR Bruker spectrometer (Vertex 70). Also, the morphologies of MCM-48 and the synthetic composites were studied by a scanning electron microscope (Gemini, Zeiss-Ultra 55) and a transmission electron microscope (JEOL-JEM2100).

4.4. Loading Properties of 5-Fluorouracil. The loading capacities as well as the main mechanisms were studied considering different factors, including (a) the loading time interval (5−1440 min), (b) the dissolved 5-Fu concentration (100−700 mg/L), (c) the pH of the drug aqueous solutions (pH 3 to pH 8), and (d) the loading temperature (30−70 °C). The mixing of the composites and the drug solutions was accomplished using a vortex rotator, and by the end of each

https://dx.doi.org/10.1021/acsomega.0c01078
ACS Omega 2020, 5, 11745−11755

test, the solutions were isolated by centrifugation and the remaining 5-Fu concentrations were measured using a UV spectrophotometer at λ_{max} = 266 nm. The loading capacities were calculated from eq 8 [25]

$$\text{loaded drug (mg/g)} = \frac{(\text{initial concentration} - \text{residual concentration}) \times \text{solvent volume}}{\text{carrier weight}} \quad (8)$$

4.5. In Vitro Release Profiles. The in vitro release properties of the investigated composites as well as MCM-48 within the gastric fluid (pH 1.2) and intestinal fluid (pH 7.4) as buffer solutions at 37.5 °C were determined for the oral formulation. During the evaluation of the tests, samples from the buffer solutions (5 mL) were collected at regular intervals to evaluate the diffused 5-Fu molecules using a UV−vis spectrophotometer at λ_{max} = 266 nm. The release percentages of 5-Fu drug were calculated from eq 9 [1]

$$\text{drug release}(\%) = \frac{\text{the amount of released 5-Fu drug}}{\text{amount of loaded 5-Fu}} \times 100 \quad (9)$$

■ ASSOCIATED CONTENT

Supporting Information

The Supporting Information is available free of charge at https://pubs.acs.org/doi/10.1021/acsomega.0c01078.

Representative equations of the studied kinetic and isotherm models (Table S1) and the obtained determination coefficients for the fitting of the results with the pharmacokinetic models (Table S2) (PDF)

■ AUTHOR INFORMATION

Corresponding Authors

Mostafa R. Abukhadra − *Geology Department, Faculty of Science and Materials Technologies and their Applications Lab, Geology Department, Faculty of Science, Beni-Suef University, Beni-Suef City 62511, Egypt;* orcid.org/0000-0001-5404-7996; Email: Abukhadra89@Science.bsu.edu.eg

Ahmed M. El-Sherbeeny − *Industrial Engineering Department, College of Engineering, King Saud University, Riyadh 11421, Saudi Arabia*; Email: aelsherbeeny@ksu.edu.sa

Authors

Nermen M. Refay − *Materials Technologies and their Applications Lab, Geology Department, Faculty of Science and Chemistry Department, Faculty of Science, Beni-Suef University, Beni-Suef City 62511, Egypt*

Mohammed A. El-Meligy − *Advanced Manufacturing Institute, King Saud University, Riyadh 11421, Saudi Arabia*

Complete contact information is available at: https://pubs.acs.org/10.1021/acsomega.0c01078

Author Contributions

This article was written through contributions of all authors. All authors have given approval to the final version of the manuscript

Notes

The authors declare no competing financial interest.

Further studies will be carried out to investigate the role of the ratio between the MCM-48 fractions and the integrated biopolymers in enhancing the loading capacities as well as the releasing properties.

■ ACKNOWLEDGMENTS

The authors extend their appreciation to the Deanship of Scientific Research at King Saud University for funding this work through research group number (RG-1440-047).

■ REFERENCES

(1) El-Zeiny, H. M.; Abukhadra, M. R.; Sayed, O. M.; Osman, A. H.; Ahmed, S. A. Insight into novel β-cyclodextrin-grafted-poly (N-vinylcaprolactam) nanogel structures as advanced carriers for 5-fluorouracil: Equilibrium behavior and pharmacokinetic modeling. *Colloids Surf., A* **2020**, *586*, No. 124197.

(2) Asgari, M.; Soleymani, M.; Miri, T.; Barati, A. A robust method for fabrication of monodisperse magnetic mesoporous silica nanoparticles with core-shell structure as anticancer drug carriers. *J. Mol. Liq.* **2019**, *292*, No. 111367.

(3) Abukhadra, M. R.; Refay, N. M.; El-Sherbeeny, A. M.; Mostafa, A. M.; Elmeligy, M. A. Facile synthesis of bentonite/biopolymer composites as low-cost carriers for 5-fluorouracil drug; equilibrium studies and pharmacokinetic behavior. *Int. J. Biol. Macromol.* **2019**, *141*, 721−731.

(4) Vatanparast, M.; Shariatinia, Z. AlN and AlP doped graphene quantum dots as novel drug delivery systems for 5-fluorouracil drug: theoretical studies. *J. Fluorine Chem.* **2018**, *211*, 81−93.

(5) Praphakar, R. A.; Jeyaraj, M.; Mehnath, S.; Higuchi, A.; Ponnamma, D.; Sadasivuni, K. K.; Rajan, M. A pH-sensitive guar gum-grafted-lysine-b-cyclodextrin drug carrier for the controlled release of 5-flourouracil into cancer cells. *J. Mater. Chem B* **2018**, *6*, 1519−1530.

(6) Tan, D.; Yuan, P.; Annabi-Bergaya, F.; Liu, D.; Wang, L.; Liu, H.; He, H. Loading and in vitro release of ibuprofen in tubular halloysite. *Appl. Clay Sci.* **2014**, *96*, 50−55.

(7) Anirudhan, T. S.; Divya, P. L.; Nima, J. Synthesis and characterization of silane coated magnetic nanoparticles/ glycidylmethacrylate-grafted-maleated cyclodextrin composite hydrogel as a drug carrier for the controlled delivery of 5-fluorouracil. *Mater. Sci. Eng., C* **2015**, *55*, 471−481.

(8) Abukhadra, M. R.; Fadl Allah, A. Synthesis and characterization of kaolinite nanotubes (KNTs) as a novel carrier for 5-fluorouracil of high encapsulation properties and controlled release. *Inorg. Chem. Commun.* **2019**, *103*, 30−36.

(9) Chandran, S. P.; Natarajan, S. B.; Chandraseharan, S.; Shahimi, M. S. B. M. Nano drug delivery strategy of 5-fluorouracil for the treatment of colorectal cancer. *J. Cancer Res. Pract.* **2017**, *4*, 45−48.

(10) Pajchel, L.; Kolodziejski, W. Synthesis and characterization of MCM-48/hydroxyapatite composites for drug delivery: Ibuprofen incorporation, location and release studies. *Mater. Sci. Eng., C* **2018**, *91*, 734−742.

(11) Shaban, M.; Abukhadra, M. R.; Hamd, A.; Amin, R. R.; Khalek, A. A. Photocatalytic removal of Congo red dye using MCM-48/Ni_2O_3 composite synthesized based on silica gel extracted from rice husk ash; fabrication and application. *J. Environ. Manage.* **2017**, *204*, 189−199.

(12) Nejat, R.; Mahjoub, A. R.; Hekmatian, Z.; Azadbakht, Tahereh. Pd-functionalized MCM-41 nanoporous silica as an efficient and reusable catalyst for promoting organic reactions. *RSC Adv.* **2015**, *5*, 16029−16035.

(13) Rehman, F.; Ahmed, K.; Rahim, A.; Muhammad, N.; Tariq, S.; Azhar, U.; Khan, A. J.; us Sama, Z.; Volpe, P. L.; Airoldi, C. Organo-bridged silsesquioxane incorporated mesoporous silica as a carrier for the controlled delivery of ibuprofen and fluorouracil. *J. Mol. Liq.* **2018**, *258*, 319−326.

(14) Jiang, M.; Hong, Y.; Gu, Z.; Cheng, L.; Li, Z.; Li, C. Preparation of a starch-based carrier for oral delivery of Vitamin E to the small intestine. *Food Hydrocolloids* **2019**, *91*, 26−33.

(15) Ji, Y.; Lin, X.; Yu, J. Preparation and characterization of oxidized starch-chitosan complexes for adsorption of procyanidins. *LWT–Food Sci. Technol.* **2020**, *117*, No. 108610.
(16) Ngah, W. W.; Teong, L. C.; Hanafiah, M. A. K. M. Adsorption of dyes and heavy metal ions by chitosan composites: A review. *Carbohydr. Polym.* **2011**, *83*, 1446−1456.
(17) Shariatinia, Z. Pharmaceutical applications of chitosan. *Adv. Colloid Interface Sci.* **2019**, *263*, 131−194.
(18) Roy, A.; Maity, P. P.; Bose, A.; Dhara, S.; Pal, S. β-Cyclodextrin based pH and thermo-responsive biopolymeric hydrogel as a dual drug carrier. *Mater. Chem. Front.* **2019**, *3*, 385−393.
(19) Carneiro, S. B.; Duarte, C.; Ílary, F.; Heimfarth, L.; Quintans, S.; de Souza, J.; Quintans-Júnior, L. J.; Veiga Júnior, V. F. D.; Neves de Lima, Á.A. Cyclodextrin−drug inclusion complexes: In vivo and in vitro approaches. *Int. J. Mol. Sci.* **2019**, *20*, 642.
(20) Hong, S.; Li, Z.; Li, C.; Donga, C.; Shuang, S. β-Cyclodextrin grafted polypyrrole magnetic nanocomposites toward the targeted delivery and controlled release of doxorubicin. *Appl. Surf. Sci.* **2018**, *427*, 1189−1198.
(21) Hou, X.; Zhang, W.; He, M.; Lu, Y.; Lou, K.; Gao, F. Preparation and characterization of β-cyclodextrin grafted N-maleoyl chitosan nanoparticles for drug delivery. *Asian J. Pharm. Sci.* **2017**, *12*, 558−568.
(22) Li, Z.; Zhang, B.; Jia, S.; Ma, M.; Hao, J. Novel supramolecular organogel based on β-cyclodextrin as a green drug carrier for enhancing anticancer effects. *J. Mol. Liq.* **2018**, *250*, 19−25.
(23) Dardir, F. M.; Mohamed, A. S.; Abukhadra, M. R.; Ahmed, E. A.; Soliman, M. F. Cosmetic and pharmaceutical qualifications of Egyptian bentonite and its suitability as drug carrier for Praziquantel drug. *Eur. J. Pharm. Sci.* **2018**, *115*, 320−329.
(24) Vardast, N.; Haghighi, M.; Dehghani, S. Sono-dispersion of calcium over AlMCM-41 used as a nanocatalyst for biodiesel production from sunflower oil: influence of ultrasound irradiation and calcium content on catalytic properties and performance. *Renewable Energy* **2019**, *132*, 979−988.
(25) Zhang, H.; Sun, H.; Zhang, D.; Zhang, W.; Chen, S.; Li, M.; Liang, P. Nanoconfinement of Ag nanoparticles inside mesoporous channels of MCM-41 molecule sieve as a regenerable and H_2O resistance sorbent for Hg0 removal in natural gas. *Chem. Eng. J.* **2019**, *361*, 139−147.
(26) Mina, J.; Valadez-Gonzalez, A.; Herrera-Franco, P.; Zuluaga, F.; Delvasto, S. Physicochemical characterization of natural and acetylated thermoplastic cassava starch. *Dyna* **2011**, *78*, 174−182.
(27) Abdullah, A. H. D.; Chalimah, S.; Primadona, I.; Hanantyo, M. H. G. Physical and chemical properties of corn, cassava, and potato starchs. *IOP Conf. Ser. Earth Environ. Sci.* **2018**, *160*, No. 012003.
(28) Lomelí-Ramírez, M. G.; Kestur, S. G.; Manríquez-González, R.; Iwakiri, S.; de Muniz, G. B.; Flores-Sahagun, T. S. Bio-composites of cassava starch-green coconut fiber: Part II—Structure and properties. *Carbohydr. Polym.* **2014**, *102*, 576−583.
(29) Geng, Q.; Li, T.; Wang, X.; Chu, W.; Cai, M.; Xie, J.; Ni, H. The mechanism of bensulfuron-methyl complexation with β-cyclodextrin and 2-hydroxypropyl-β-cyclodextrin and effect on soil adsorption and bio-activity. *Sci. Rep.* **2019**, *9*, No. 1882.
(30) Stopilha, R. T.; Xavier-Júnior, F. H.; De Vasconcelos, C. L.; Fonseca, J. L. Carboxymethylated-β-cyclodextrin/chitosan particles: bulk solids and aqueous dispersions. *J. Dispersion Sci. Technol.* **2019**, 1−8.
(31) Kevadiya, B. D.; Patel, T. A.; Jhala, D. D.; Thumbar, R. P.; Brahmbhatt, H.; Pandya, M. P.; Rajkumar, S.; Jena, P. K.; Joshi, G. V.; Gadhia, P. K.; Tripathi, C. B. Layered inorganic nanocomposites: a promising carrier for 5-fluorouracil (5-FU). *Eur. J. Pharm. Biopharm.* **2012**, *81*, 91−101.
(32) Tu, Y.; Feng, P.; Ren, Y.; Cao, Z.; Wang, R.; Xu, Z. Adsorption of ammonia nitrogen on lignite and its influence on coal water slurry preparation. *Fuel* **2019**, *238*, 34−43.
(33) Rajabi, M.; Mirzab, B.; Mahanpoorc, K.; Mirjalilid, M.; Najafi, F.; Moradif, O.; Sadegh, H.; Shahryari-ghoshekandi, R.; Asif, M.; Tyagi, I.; Agarwal, S.; Gupta, V. K. Adsorption of malachite green from aqueous solution by carboxylate group functionalized multi-walled carbon nanotubes: Determination of equilibrium and kinetics parameters. *J. Ind. Eng. Chem.* **2016**, *34*, 130−138.
(34) Liu, Y.; Yan, C.; Zhao, J.; Zhang, Z.; Wang, H.; Zhou, S.; Wu, L. Synthesis of zeolite P1 from fly ash under solvent-free conditions for ammonium removal from water. *J. Cleaner Prod.* **2018**, *202*, 11−22.
(35) Goscianska, J.; Olejnik, A.; Nowak, I.; Marciniak, M.; Pietrzak, R. Ordered mesoporous silica modified with lanthanum for ibuprofen loading and release behaviour. *Eur. J. Pharm. Biopharm.* **2015**, *94*, 550−558.
(36) Rehman, F.; Ahmed, K.; Rahim, A.; Muhammad, N.; Tariq, S.; Azhar, U.; Khan, A. J.; us Sama, Z.; Volpe, P. L.; Airoldi, C. Organo-bridged silsesquioxane incorporated mesoporous silica as a carrier for the controlled delivery of ibuprofen and fluorouracil. *J. Mol. Liq.* **2018**, *258*, 319−326.
(37) Sun, L.; Chen, Y.; Zhou, Y.; Guo, D.; Fan, Y.; Guo, F.; Zheng, Y.; Chen, W. Preparation of 5-fluorouracil-loaded chitosan nanoparticles and study of the sustained release in vitro and in vivo. *Asian J. Pharm. Sci.* **2017**, *12*, 418−423.
(38) Dziadkowiec, J.; Mansa, R.; Quintela, A.; Rocha, F.; Detellier, C. Preparation, characterization and application in controlled release of Ibuprofen-loaded Guar Gum/Montmorillonite Bionanocomposites. *Appl. Clay Sci.* **2017**, *135*, 52−63.
(39) Arifin, D. Y.; Lee, L. Y.; Wang, C. H. Mathematical modeling and simulation of drug release from microspheres: Implications to drug delivery systems. *Adv. Drug Delivery Rev.* **2006**, *58*, 1274−1325.
(40) Gouda, R.; Baishya, H.; Qing, Z. Application of mathematical models in drug release kinetics of carbidopa and levodopa ER tablets. *J. Dev. Drugs* **2017**, *6*, No. 171.
(41) Ramteke, K. H.; Dighe, P. A.; Kharat, A. R.; Patil, S. V. Mathematical models of drug dissolution: a review. *Scholars Acad. J. Pharm.* **2014**, *3*, 388−396.

https://dx.doi.org/10.1021/acsomega.0c01078
ACS Omega 2020, 5, 11745−11755